

Research Article

Cite this article: Zhu M, Wei R, Li J, Bao J, Wei L, Yu X, Zhou Z, Hu F, Li S (2025) Protective mechanism of milk-derived bioactive peptides VPP and IPP against lipopolysaccharide-induced inflammation in bovine mammary epithelial cells and a mouse mastitis model. *Animal Nutriomics* **2**, e10, 1–13. <https://doi.org/10.1017/anr.2025.1>

Received: 28 June 2024

Revised: 8 December 2024

Accepted: 15 January 2025

Keywords:

VPP; IPP; BMEC; mastitis; blood–milk barrier; PI3K/AKT; fibronectin

Corresponding author: Shanshan Li;

Email: lishanshan@zju.edu.cn

Protective mechanism of milk-derived bioactive peptides VPP and IPP against lipopolysaccharide-induced inflammation in bovine mammary epithelial cells and a mouse mastitis model

Meifei Zhu¹ , Ruike Wei¹, Jingyan Li¹, Jiayi Bao¹, Lin Wei¹, Xinyu Yu¹, Zheng Zhou², Fuliang Hu¹ and Shanshan Li¹ 

¹College of Animal Sciences, Zhejiang University, Hangzhou, P. R. China and ²Department of Animal Science, Michigan State University, East Lansing, MI, USA

Abstract

Bovine mastitis harms milk quality and cattle health. Val-Pro-Pro (VPP) and Ile-Pro-Pro (IPP) are well-known milk-derived bioactive peptides with anti-inflammatory activity. However, the impact of VPP and IPP on mastitis remain unknown. This study aimed to investigate the anti-inflammatory effects and the underlying mechanisms of VPP and IPP in lipopolysaccharide (LPS)-induced inflammation. When cells were treated with LPS (1 µg/mL) for 24 h, the protein levels of pro-inflammatory factors (tumor necrosis factor-α (TNF-α), interleukin(IL)-1β and IL-6)) and chemokine (monocyte chemoattractant protein-1 (MCP-1)) were markedly increased, and the protein level of anti-inflammatory cytokine (IL-10) was reduced. Both VPP and IPP with concentrations of 50 and 100 µM reversed these phenomena and further inhibited the protein expression of β-casein induced by LPS. In a mouse mastitis model, different concentrations of VPP and IPP (300, 600 µM/kg) pretreatment alleviated histopathological lesions in the mammary gland and suppressed the mRNA expression of *TNFα*, *IL1β*, and *IL6* induced by LPS. VPP and IPP also maintained the integrity of the blood–milk barrier in mice. RNA-seq analyses indicated that enriched phosphatidylinositol 3-kinase/protein kinase B (PI3K/AKT) and mitogen-activated protein kinase (MAPK) signaling pathways likely contribute to the changes observed ($P < 0.05$ and $|\log_2 \text{fold change (FC)}| \geq 1$). Notably, fibronectin was identified as an important hub by protein–protein interaction (PPI) analysis and molecular docking combined with molecular dynamics simulation. In summary, VPP and IPP exerted a protective effect on LPS-induced inflammation by regulating PI3K/AKT signaling pathway via fibronectin.

Introduction

Cow mastitis, with a global incidence of up to 50% (Sharun et al. 2021), is an inflammation of the mammary tissue triggered by pathogenic infection, mechanical injury, and environmental factors. Mastitis not only has the potential to harm the health of cows but can also affect the quality of milk, resulting in significant financial losses in the dairy sector (Li et al. 2021). *Escherichia coli*, a type of Gram-negative bacteria, is a prevalent cause of acute mastitis. Endotoxin lipopolysaccharide (LPS) of *E. coli* induces the secretion of inflammatory factors including TNF-α, IL-6, IL-1β from the breast gland (Ran et al. 2020; Yin et al. 2021). Although antibiotics can be used to treat mastitis, residues of antibiotics may compromise milk yield and quality and give rise to antibiotic resistance. Therefore, an alternative nutritional strategy is desired to reduce mastitis-induced inflammation in dairy cows.

Val-Pro-Pro (VPP) and Ile-Pro-Pro (IPP) are tripeptides obtained from milk that were originally recognized as inhibitors of angiotensin I-converting enzyme and exerted antihypertension activity (Nakamura et al. 1995). VPP is located at fragments of 84–86 in β-casein, while IPP exists at fragments of 74–76 of β-casein and 108–110 of κ-casein (Li et al. 2019). These two milk-derived tripeptides also exhibited anti-inflammation function both *in vivo* and *in vitro* (Sawada et al. 2015; Chakrabarti and Wu, 2015). For example, VPP and IPP were observed to prevent TNFα-induced loss of adiponectin through inhibiting the initiation of the nuclear factor kappa B (NF-κB) in 3T3-F442A murine pre-adipocytes. In vascular smooth muscle cells, VPP exerted anti-inflammatory activity via diminishing the initiation of extracellular signal-regulated kinases (ERK)1/2 to protect vascular function (Chakrabarti and Wu, 2015; Chakrabarti et al. 2017). Additionally, VPP was found to decrease the activity of

© The Author(s), 2025. Published by Cambridge University Press on behalf of Zhejiang University and Zhejiang University Press. This is an Open Access article, distributed under the terms of the Creative Commons Attribution licence (<http://creativecommons.org/licenses/by/4.0>), which permits unrestricted re-use, distribution and reproduction, provided the original article is properly cited.

pro-inflammatory genes (i.e. *TNF α* and *IL1 β*) in mice that were made obese by their diet (Sawada et al. 2015). Although these findings support an anti-inflammatory effect of VPP and IPP, it is still unclear whether VPP and IPP can alleviate mastitis in dairy cows through their anti-inflammatory activity, and the specific mechanisms involved are yet to be determined. We hypothesize that VPP and IPP have the anti-inflammatory activity in mammary gland of dairy cow. Therefore, this study aimed to evaluate the role of VPP and IPP against LPS-induced inflammation in bovine mammary epithelial cells (BMECs) and a mouse model of mastitis. Our study will provide new insight in the application of milk-derived anti-inflammatory peptides in lactating cows.

Material and methods

Reagents

VPP and IPP were obtained from ChinaPeptides Co., Ltd (Shanghai, China). LPS (*E.coli* O111:B4), collagenase I and II were purchased from Sigma-Aldrich (St. Louis, MO, USA). Fetal bovine serum was obtained from Gibco (Grand Island, NY, USA). Enzyme-linked immunosorbent assay (ELISA) kits for TNF- α , IL-6, IL-1 β , MCP-1, and IL-10 were purchased from Shanghai Yu Bo Biotech Co., Ltd (Shanghai, China). The primary antibodies β -tubulin were purchased from Beyotime Biotechnology (Shanghai, China). The primary antibodies ZO-1 and Occludin and the secondary antibodies used in this study including rabbit monoclonal antibodies and mouse monoclonal antibodies were purchased from Abcam (Cambridge, UK).

Cell culture and treatment

The procedures for the isolation and culture of primary BMECs were described as reported previously (Lin et al. 2018). In brief, the small pieces of mammary gland were incubated with 0.25% trypsin at 37°C for 30 min in the dark, and then the digested sediments were incubated with 1 mg/mL of the mixture of collagenase I and II with the ratio of 1:1 at 37°C for 4 h to separate BMECs and fibroblasts. The dispersed BMECs were cultured in α -Minimum Essential Medium (α -MEM, HyClone, Logan, UT) supplemented with 1% penicillin/streptomycin solution in a humidified incubator with 5% CO₂ at 37°C.

BMECs were treated with various concentrations of LPS (0, 0.1, 1, 10, 100 μ g/mL) for 24 h to assess the impact of LPS-induced cells on viability and inflammatory response.

Based on the above results of LPS concentration (1 μ g/mL), cells were further pretreated with various concentrations of VPP or IPP (25, 50, 100 μ M) for 2 h and then exposed to 1 μ g/mL LPS for 24 h to assess the protective effect of VPP and IPP on inflammatory response, cell death and β -casein expression.

Cell viability assay

Cell viability assay was performed using the Cell Counting Kit-8 (CCK-8) kit (Beyotime, Shanghai, China) by the instructions provided by the manufacturer. In summary, 96-well culture plates were seeded with 5000 BMECs and incubated in an incubator that was humidified with 5% CO₂ at 37°C for 24 h. Different concentrations of LPS were added for 24 h in a trial. Various concentrations of VPP or IPP were pretreated for 2 h and then activated with LPS (1 μ g/mL) for 24 h in a separate experiment. Afterward, a volume of

10 μ L of CCK-8 was introduced into each well and allowed to incubate for a duration of 2 h. Subsequently, the absorbance (optical density [OD]) was quantified at a wavelength of 450 nm using the BioTek SYNERGY HTX multi-mode microplate reader (BioTek, USA).

Cell apoptosis assay

The apoptosis cells were detected with Annexin V-FITC/PI apoptosis detection kit (BestBio, Nanjing, China). The cells were harvested using trypsin solution without EDTA and then subjected to centrifugation at a speed of 1500 revolutions per minute for 5 min at ambient temperature. After being rinsed twice with PBS, the cells were resuspended in 300 μ L of 1 \times binding buffer. The cells were treated with 5 μ L of Annexin V-FITC for 15 min and thereafter exposed to 10 μ L of PI for another 15 min at room temperature in the absence of light. Ultimately, the levels of cell apoptosis were examined using flow cytometry (Becton Dickinson Company, NJ, USA).

Enzyme-linked immunosorbent assay

The protein levels of pro-inflammatory factors (TNF- α , IL-6, IL-1 β), chemokine (MCP-1), anti-inflammatory factor (IL-10) in BMECs were determined using an ELISA kit following the instructions provided by the manufacturer (Shanghai Yu Bo Biotech Co., Ltd, Shanghai, China).

Western blot analysis

Proteins were recovered from BMECs utilizing a radioimmuno-precipitation assay lysis buffer including a proteinase inhibitor (PMSF, Beyotime). Protein concentration was determined by BCA Protein Assay Kit. Proteins, with a quantity of 20 μ g, were isolated by sodium dodecyl sulfate-polyacrylamide gel electrophoresis and then deposited onto the polyvinylidene difluoride (PVDF) membranes. The membranes were obstructed with blocking buffer for 2 h. Then, the PVDF membrane was exposed to the primary antibodies (β -casein or β -tubulin) at 4°C overnight followed by exposure to the secondary antibody (goat anti-rabbit (1:5000) antibody) for 1 h at room temperature. The presence of immunopositive bands was detected using enhanced chemiluminescence (Bio-Rad, CA, USA).

Mice and treatments

BALB/c mice (8–9 weeks old, 20–25 g weight) were obtained from the Animal Experimental Center of Zhejiang Chinese Medical University (Hangzhou, China) and distributed in a small cage with two females and one male kept under a standard condition (12 h light-dark cycle, 22–23°C). Individual cages were provided for pregnant female mice, who were then exposed to various treatments. Forty-two nursing mice were allocated randomly into seven groups ($n = 6$ per group): Control, LPS (0.2 mg/mL, 50 μ L), LPS + VPP (300, 600 μ M/kg/d), LPS + IPP (300, 600 μ M/kg/d), and LPS + dexamethasone (DEX) (5 mg/kg/d). The dosages of LPS, VPP or IPP were based on the previous study (Liu et al. 2023; Ran et al. 2022). Prior to receiving LPS treatment on days 5–9 of lactation, the mice were gavaged VPP, IPP, and DEX for 5 days, whereas control and LPS-induced groups were gavaged with an equivalent amount of sterile saline. On day 9 of lactation, 1 h after

gavage of VPP, IPP, DEX or saline, the mice were administered LPS by injecting it into their fourth mammary ducts using a microsyringe equipped with a 32-G needle. Twenty-four hours after the LPS injection, all of the mice were euthanized, and samples of mammary tissue were obtained for further studies.

Hematoxylin–eosin staining

The mammary gland tissues were immersed in a solution of 4% paraformaldehyde for a duration exceeding 24 h to fix them. The tissues were fixed in paraffin and then cut into pieces that were 5 μ m thick. To assess histological alterations, the tissues were stained with haematoxylin–eosin (H&E) and examined using a microscope (NIKON ECLIPSE CI, Nikon, Tokyo Metropolis, Japan).

RNA extraction and real-time PCR analysis

Total RNA was extracted by the RNA Pure Kit (Accurate Biotechnology, Changsha, China) according to the manufacturer's instructions. The cDNA was transcribed using the PrimeScript RT Reagent Kit (Accurate Biotechnology, Changsha, China). Quantitative real-time PCR was performed using SYBR[®] Green Pro Taq HS (Accurate Biotechnology, Changsha, China) by a StepOnePlus[™] real-time PCR detection system (Applied Biosystems, Waltham, MA, USA). Given the robust stability of β -actin (*ACTB*) gene expression and the absence of differential expression in the RNA-seq analysis, data normalization was performed using β -actin as an internal reference gene, and the relative gene expression values were determined using the $2^{-\Delta\Delta CT}$ technique (Wan et al. 2021). The primer sequences employed in this investigation are enumerated in Table 1, and RNA quality was shown in Table 2.

Immunofluorescence analysis

The mammary gland samples were immersed in 4% paraformaldehyde for fixation and subsequently fixed in paraffin. The mammary gland that was embedded was sliced into paraffin sections that were 3 μ m thick. The sections of the mammary gland were treated with xylene to remove the paraffin and prepare them for antigen retrieval. The sections of the mammary gland were treated with 5% donkey serum at room temperature for 1 h, followed by incubation with primary antibodies (ZO-1 and Occludin) at 4°C overnight. Subsequently, slices of the mammary gland were stained using a goat anti-rabbit HRP-linked secondary antibody at room temperature for 1 h. Ultimately, sections of the mammary gland were stained with DAPI as a counterstain, and the resulting images were examined using a fluorescence microscope (NIKON ECLIPSE CI, Nikon, Tokyo Metropolis, Japan).

Transcriptome analysis

The total RNA of mammary gland samples was isolated using Trizol extraction methods. The purity and concentration of the extracted RNA samples were determined by a NanoDrop 2000 spectrophotometer (Thermo Fisher Scientific, Waltham, MA, USA). The library was constructed using the NEBNext[®] Ultra[™] RNA Library Prep Kit for Illumina[®] (NEB, USA, Catalog #: E7530L) following the manufacturer's instructions. The samples were sequenced on the illumina novaseq 6000 (illumina, CA, USA).

Table 1. Primers Used for qRT-PCR

gene	sequence
Mouse TNF- α	F: CATCTTCTCAAATTCGAGTGACAA R: TGGGAGTAGACAAGGTACAACCC
Mouse IL-1 β	F: CCGTGGACCTTCCAGGATGA R: GGGAAAGTCCACACACCAGCA
Mouse IL-6	F: TAGTCCTTCTACCCCAATTTCC R: TTGGTCTTAGCCACTCCTTC
Mouse Occludin	F: TCTGCTTCATCGTTCCTTAG R: GTCGGTTCACTCCCATTA
Mouse ZO-1	F: ACTCCACTTCCCCAAAAC R: CCACAGCTGAAGGACTCACA
Mouse β -actin	F: GTGACGTTGACATCCGTAAGA R: GCCGGACTCATCGTACTCC
Mouse Itgb3	F: TGGAAGGCTGGCAGGCATTG R: TGGTAGTGGAGGCAGAGTAGTGG
Mouse Pgf	F: TGGAGACGACAAAGGCAGAAAGG R: ACGGGTGGGGTTCCTCAGTC
Mouse Csf3	F: GCCATGCCAGCCTTCACTTC R: GCGAGCCGTCTCCAGGAAG
Mouse Ereg	F: TCAGCACAAACCGTATCCCATC R: AAGCAGTAGCCGTCATGTCAG
Mouse Csf3r	F: CGTGGTGTGAGAAGAAGCAACTAG R: GGAAGTCCAGGACAGCAGGTAG
Mouse Osm	F: CGGCACAATATCCTCGGCATAAG R: TGGTGTGTAGTGGACCGTGAG
Mouse Pik3r6	F: TGCTCACACTATGGCTGGACAAG R: TCTCTGCCCGTGCGAATTG
Mouse Fn1	F: CACCGACGAAGGCCCTTACAG R: CCTTGTGCCTCTCTGGTTCTG
Mouse Pck1	F: AACTGTTGGCTGGCTCTCACTG R: GGATGGGCACTGTGTCTCTCTG
Mouse Col9a1	F: AGCCAGGAAGACAAGGACACAAG R: GCCAGTGATGCCTCTCAGACC
Mouse Pik3cg	F: CGCATCAGCAAGACTCCAGAAAC R: GGTAGAAGTCCGAGCCACAC

The clean data were obtained by eliminating the linker sequence and low-quality sequence from raw data, which was assessed for quality using FASTQC. Differential expression analysis was performed using DESeq2 (Bioconductor version 1.6.3), and gene expression with the threshold of $P_{adj} < 0.05$ (followed an FDR correction) and the absolute value of $|\log_2 \text{fold change (FC)}| \geq 1$ among two groups were regarded as the differentially expressed genes (DEGs). The selected DEGs were confirmed by RT-PCR.

Gene Ontology analysis encompassing biological process, molecular function, and cellular component was conducted by GOSeq (v1.34.1) with a significant Adj. p value < 0.05 . KEGG (Kyoto Encyclopedia of Genes and Genomes) was implemented by clusterProfiler 3.8.1. The PPI networks of the DEGs were performed with STRING database (<http://string-db.org/>) with high confidence (0.7) and drawn with Cytoscape V3.9.1 software.

Table 2. RNA quality assay

Sample (mice)	concentration (ng/ μ L)	OD260/OD280
CON-1	1340	2.01
CON-2	1602	2.02
CON-3	1109	2.01
LPS-1	614	2.03
LPS-2	824	2.02
LPS-3	596	2.06
LPS+VPP (300 μ M/kg)-1	664	2.07
LPS+VPP (300 μ M/kg)-2	709	2.03
LPS+VPP (300 μ M/kg)-3	849	2.04
LPS+VPP (600 μ M/kg)-1	634	2.02
LPS+VPP (600 μ M/kg)-2	604	2.06
LPS+VPP (600 μ M/kg)-3	600	2.07
LPS+IPP (300 μ M/kg)-1	649	2.02
LPS+IPP (300 μ M/kg)-2	668	2.02
LPS+IPP (300 μ M/kg)-3	709	2.03
LPS+IPP (600 μ M/kg)-1	800	2.04
LPS+IPP (600 μ M/kg)-2	1037	2.01
LPS+IPP (600 μ M/kg)-3	1345	2.03
LPS+DEX-1	459	2.03
LPS+DEX-2	706	2.04
LPS+DEX-3	668	2.02

Molecular docking

The 3D structure of fibronectin was acquired from Uniprot (<https://www.uniprot.org/>), and the 3D structure of VPP and IPP were obtained from Pubchem (<https://pubchem.ncbi.nlm.nih.gov/>). The molecular docking of VPP or IPP with fibronectin was simulated using Autodock 4, and the docking time was 10. Finally, the results of protein-ligand complex were displayed using PyMOL Molecular Graphics System (Version 2.0 Schrodinger, LLC.)

Molecular dynamics simulation

The stability of VPP–fibronectin and IPP–fibronectin complexes were assessed with Gromacs version 2022.2 software package with Amber99sb-ildn force filed. VPP–fibronectin and IPP–fibronectin complexes were inserted into a regularly shaped cubic container, and a TIP3P water model was included in the container to dissolve the complexes. To neutralize the charge, a sufficient amount of Na⁺ was introduced into the system. Subsequently, the simulation underwent energy minimization. The long-range interactions were evaluated using the Particle Mesh Ewald approach. A 12 Å cutoff was employed to handle van der Waals interactions. The Linear Constraint Solver (LINCS) method was employed to restrict all hydrogen-related bonds. The Canonical Ensemble (NVT) and Isothermal-Isobaric Ensemble (NPT) ensembles were used to achieve thermal equilibrium in the systems for 100 ps. Temperature and pressure coupling in Molecular Dynamics (MD) ensembles were accomplished by employing a V-rescale thermostat and a Parrinello–Rahman barostat, respectively.

Statistical analysis

All data are expressed as the mean \pm SEM. Statistical significance was indicated by asterisks and hash symbols (* p < 0.05, ** p < 0.01; # p < 0.05, ## p < 0.01). For the cell trials, the differences in the cell viability, apoptosis, the expression of inflammatory cytokines and β -casein between the control group, LPS group, and different concentrations of VPP and IPP groups were compared. For the animal trials, the differences in the expression of inflammatory cytokines and tight junction proteins in the control group, LPS group, VPP and IPP groups with concentrations of 300 and 600 μ M/kg were compared. In both cell and animal trials, when the data test was normally distributed, the distinctions among the various experimental groups were examined using a one-way ANOVA and Student–Newman–Keuls multiple comparison test in SPSS (version20, IBM Corp, Armonk, NY, USA). On the other hand, when the data were not normally distributed, the differences were examined using the Kruskal–Wallies test and Dunn's multiple comparison test.

Results

Effects of VPP and IPP on alleviating inflammatory response in LPS-induced BMECs

To investigate the effect of LPS on BMECs, the cells were treated with different concentrations of LPS (0–100 μ g/mL) for 24 h. A dose-dependent inhibition of cell survival by LPS was observed (Fig. 1A). The expression of pro-inflammatory cytokines (TNF- α , IL-1 β , IL-6) and chemokine (MCP-1) increased after treatment with LPS in a dose-dependent manner, while the expression of anti-inflammatory cytokine (IL-10) was decreased when the treatment concentration of LPS was more than 1 μ g/mL (Fig. 1B–F). Given the inflammatory response, 1 μ g/mL of LPS was selected to assess the anti-inflammatory effects of VPP and IPP in BMECs.

Supplementation of VPP or IPP at concentrations of 50 and 100 μ g/mL significantly reversed the decrease in BMECs viability induced by LPS. Compared with LPS stimulation, pretreatment with both VPP and IPP significantly inhibited the expression of pro-inflammatory cytokines (TNF- α , IL-1 β , IL-6) and chemokine (MCP-1), while enhancing the expression of anti-inflammatory cytokine (IL-10) (Fig. 1H–L).

Effects of VPP and IPP on death and β -casein expression in LPS-induced BMECs

As shown in Fig. 2A–B, VPP and IPP downregulated the increased cell apoptosis stimulated by LPS treatment at concentrations from 25 to 100 μ M by 7.77% and 8.53%, 16.93% and 18.65%, 23% and 24.4%, respectively. Furthermore, western blot analysis revealed that VPP and IPP pretreatment at a concentration of 50 μ M rescued the expression of β -casein in LPS-induced BMECs (Fig. 2C). The accumulating results suggest an anti-inflammatory effect of VPP and IPP on LPS-induced BMECs.

Effects of VPP and IPP on alleviating LPS-induced mammary inflammatory response in mice

As shown in Fig. 3B, H&E staining results showed hyperemia oedema and a high level of neutrophil infiltration in the mammary tissue acini in the LPS group compared to the control.

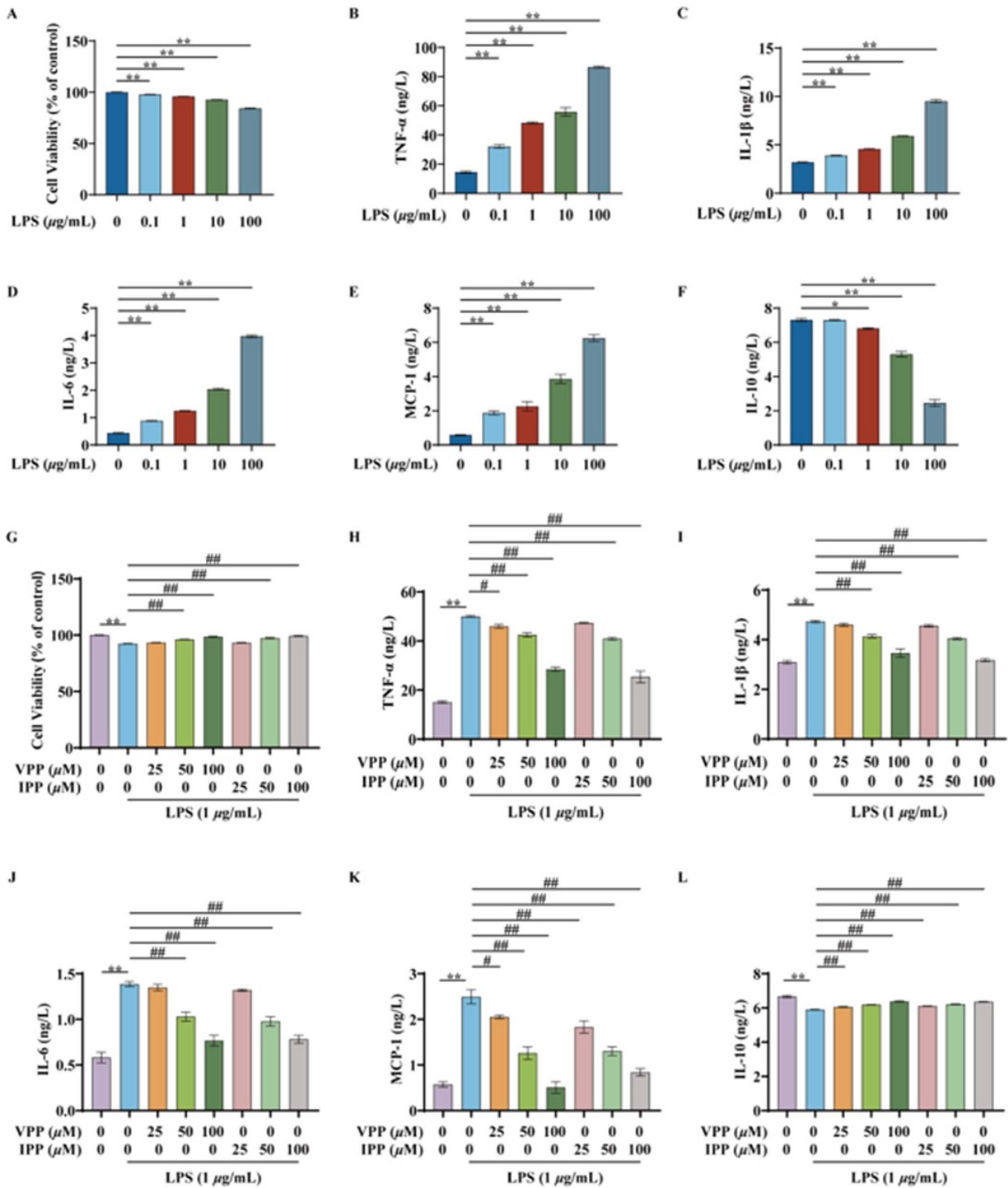


Figure 1. Both VPP and IPP ameliorated inflammatory response in LPS-induced bMECs. BMECs were treated with different dosages of LPS (0, 0.1, 1, 10 and 100 μg/ml) for 24 h. (A) Cell viability was determined with a CCK-8 kit, and the concentrations of (B) TNF-α, (C) IL-1β, (D) IL-6, (E) MCP-1 and (F) IL-10 in the cell medium were estimated by ELISA. bMECs were pretreated with different concentrations of VPP and IPP (25, 50, 100 μM) for 2 h following by LPS (1 μg/ml) challenge for 24 h. (G) Effects of VPP and IPP on LPS-induced cell viability. the concentration of (H) TNF-α, (I) IL-1β, (J) IL-6, (K) MCP-1 and (L) IL-10 within LPS-stimulated MACT cells were analyzed by ELISA. Data are represented as mean ± SEM (n = 3). *p < 0.05 and **p < 0.01 compared with the untreated group; #p < 0.05 and ##p < 0.01 compared with the LPS group.

Nevertheless, the gavage of VPP, IPP and the positive control (DEX) considerably diminished the degenerative alterations of these mammary gland tissues in the mice (Fig. 3B). Moreover,

VPP, IPP, and DEX significantly inhibited the expression of pro-inflammatory cytokines (*TNFα*, *IL1β*, *IL6*) induced by LPS (Fig. 3C-E).

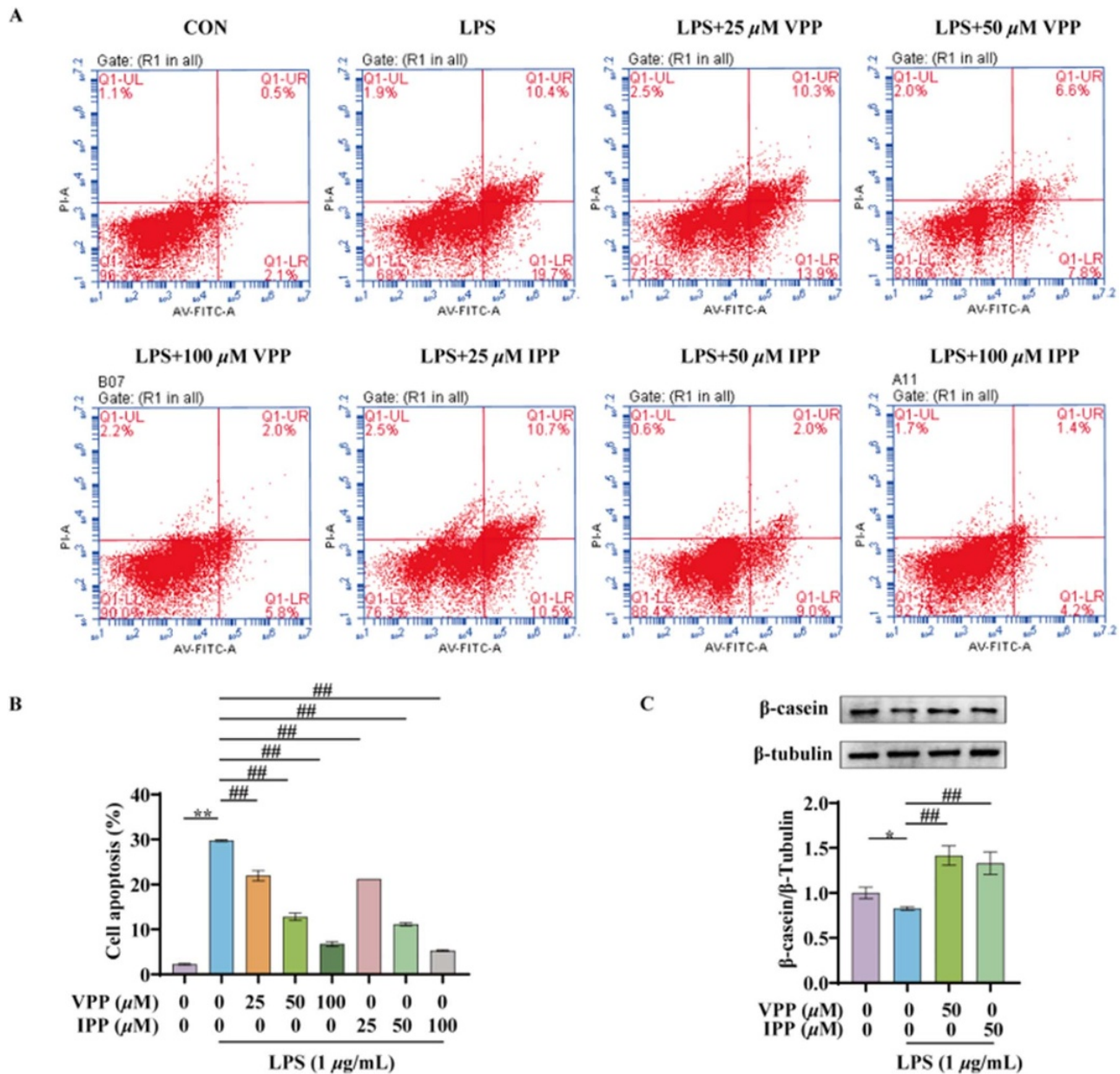


Figure 2. Effects of VPP and IPP on death and β -casein expression in LPS-induced BMECs. BMECs were pretreated with different concentrations of VPP and IPP (25, 50, 100 μ M) for 2 h, following by LPS (1 μ g/ml) challenge for 24 h. (A) Flow cytometry analysis of annexin V/FITC/PI staining cells. (B) Quantification of the total cell apoptotic rates. (C) The protein levels of β -casein were measured by western blot and quantified by comparison with β -tubulin. Data are represented as mean \pm SEM ($n = 3$). * $p < 0.05$ and ** $p < 0.01$ compared with the control group; # $p < 0.05$ and ## $p < 0.01$ compared with the LPS group.

Effects of VPP and IPP on maintaining the integrity of the blood-milk barrier

As immunofluorescence results shown in Fig. 4A, VPP and IPP significantly reversed the reduced expression of occludin and ZO-1, as well as alleviated the disorder of tissue distribution stimulated by LPS in mice. These phenomena were also validated by the mRNA expression of *occludin* and *ZO1* treated with VPP and IPP (Fig. 4B–C), suggesting that VPP and IPP could maintain the integrity of the junction complex by promoting the expression of tight junction proteins.

Transcriptome analysis of DEGs modified by VPP or IPP in the mammary gland of mice

RNA-seq analysis showed that the mammary transcriptome profiles of the control, LPS, LPS with addition of VPP (600 μ M/kg) or IPP (600 μ M/kg) groups were distinct from different treatments and highly reproducible among each groups (Figure 5A and 5C, 6A and 6C). A total of 741 DEGs including 156 upregulated genes and 585 downregulated genes were identified in the VPP groups, while 797 DEGs involving in 280 upregulated genes and 517 downregulated genes were identified in the IPP groups compared to the LPS group (Figs 5B and 6B). The DEGs in the VPP group were mainly enriched in the inflammation-related pathways

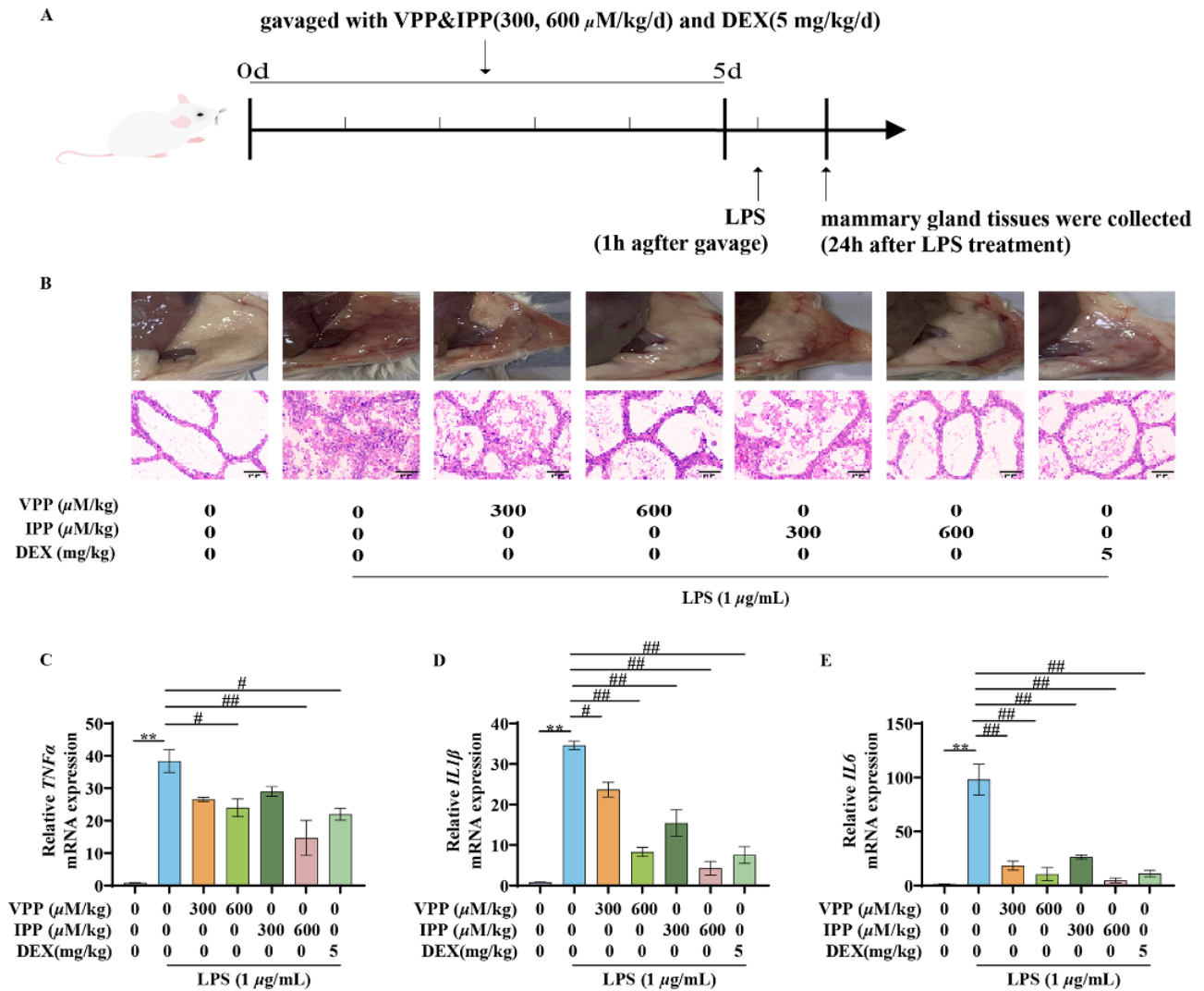


Figure 3. VPP and IPP alleviate LPS-induced mammary inflammatory response in mice. (A) Flow chart of mice experiment. (B) Representative images of mammary gland stained with H&E in mice (bar = 50 μ m). (C–E) Qrt-pcr analysis of mammary gland tissue from 3 mice for each group to determine expression of inflammatory factors. data are represented as mean \pm SEM ($n = 3$). * $p < 0.05$ and ** $p < 0.01$ compared with the control group; # $p < 0.05$ and ## $p < 0.01$ compared with the LPS group.

including PI3K-AKT and MAPK pathways. These inflammation-related pathways might be responsible for the protective effect of VPP in this study (Fig. 5D). The KEGG enriched in the IPP group was similar to the VPP vs. LPS group (Fig. 6D). In addition, the qPCR results indicated the changes in the expression of selected DEGs related to PI3K-AKT signaling pathways (Fig. 5E–F and Fig. 6E–F).

Both VPP and IPP alleviated inflammation by interacting with fibronectin in PI3K-AKT signaling pathway

The genes enriched in PI3K-AKT signaling pathway were analyzed by the PPI network. By accessing the degree centrality analysis of the PPI network, 11 hub genes were obtained in the VPP vs LPS group, 14 hub genes were obtained in the IPP vs LPS group (degree ≥ 10)(Fig. 7A, C). Of these, fibronectin ranked highest in both VPP and IPP compared to LPS groups. Molecular docking predicted that hydrogen bonds existed between VPP and fibronectin at the ARG-35 and GLU-80 amino acid residues with

a total energy of -5.08 kcal/mol; and hydrogen bonds existed between IPP and fibronectin at the ASP-35, ASN-1810 and GLU-99 amino acid residues with a total energy of -5.17 kcal/mol (Fig. 7B, D). Furthermore, the stability of VPP–fibronectin and IPP–fibronectin complexes was evaluated to predict the interaction between VPP/IPP and fibronectin. As shown in Fig. 7E, the root-mean-square deviation (RMSD) of VPP–fibronectin reached equilibrium after 30 ns, while IPP–fibronectin maintained equilibrium at 70 ns. The average root-mean-square fluctuation (RMSF) values of VPP–fibronectin and IPP–fibronectin complexes were 0.24 ± 0.07 and 0.35 ± 0.11 nm, respectively (Fig. 7F). The radius of gyration (Rg) values of VPP–fibronectin (2.27 ± 0.04 nm) was lower than IPP–fibronectin (2.32 ± 0.04 nm) (Fig. 7G). As shown in Fig. 7H, the number of hydrogen bonds formed in VPP–fibronectin and IPP–fibronectin complexes were 0–4 and 0–3, respectively. The results of molecular dynamics simulations suggested that both VPP–fibronectin and IPP–fibronectin complexes have stable global structure and tight binding.

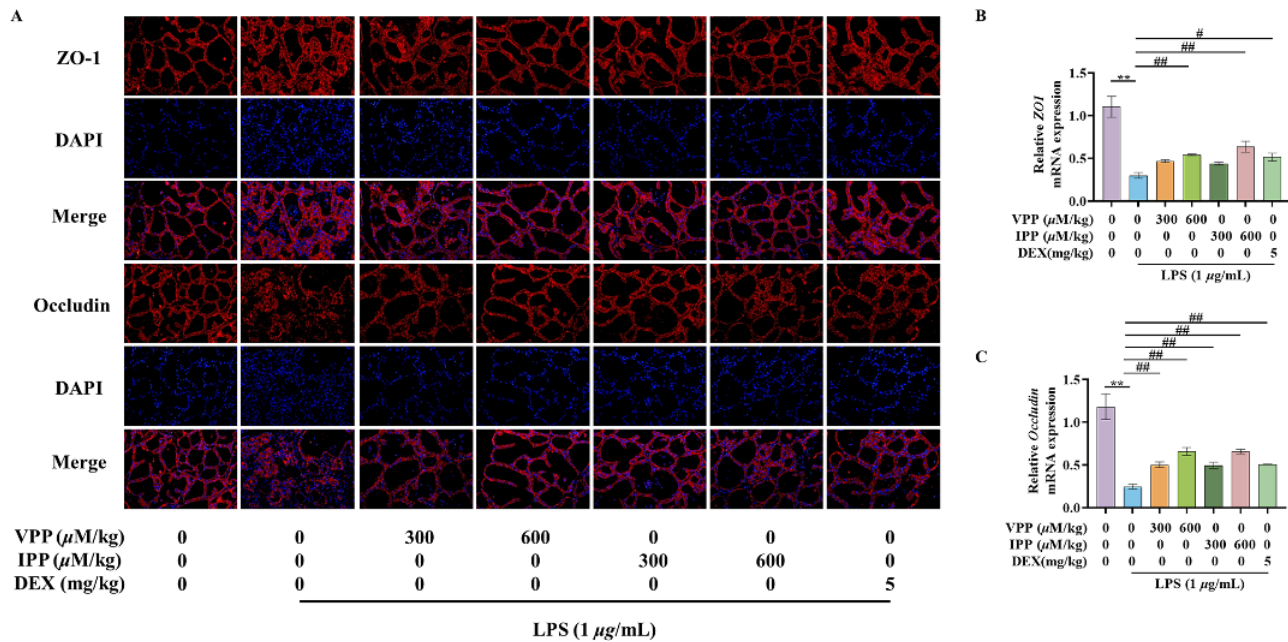


Figure 4. VPP and IPP maintain the integrity of the blood–milk barrier. (A) Immunofluorescence staining of ZO-1 and occludin (bar = 50 μm). (B) qRT-PCR analysis of mammary gland tissue from 3 mice for each group to determine expression of *ZO1* and *occludin*. Data are represented as mean \pm SEM ($n = 3$). * $p < 0.05$ and ** $p < 0.01$ compared with the control group; # $p < 0.05$ and ## $p < 0.01$ compared with the LPS group.

Discussion

Gram-negative pathogens such as *Escherichia coli* are the main cause of mastitis in dairy cows (Yang et al. 2020). LPS, a component of Gram-negative bacteria's cell wall, causes an inflammatory response during bacterial infection (Fang et al. 2021). Following an LPS challenge, the proinflammatory mediators (i.e. TNF- α , IL-6, IL-1 β) are released (Huang et al. 2022; Ashraf and Imran, 2020). We propose that bioactive tripeptides VPP and IPP originating from milk casein may act as an efficient anti-inflammatory agent to prevent mastitis. In this study, BMECs and a mastitis mouse model were applied to investigate the effect of milk-derived tripeptides VPP and IPP on LPS-stimulated inflammation. First, an inflammatory model via LPS-stimulated BMECs was established as an *in vitro* model of cow mastitis (Jiang et al. 2022). LPS could decrease cell viability and the generation of anti-inflammatory cytokine IL-10, while increasing the generation of the pro-inflammatory mediators TNF- α , IL-6, IL-1 β and the chemokine MCP-1. Both VPP and IPP reversed the negative impact on cell viability and inflammatory cytokines stimulated by LPS. Besides, VPP and IPP also reduced expression of proinflammatory cytokines *TNF α* , *IL1 β* , and *IL6* in LPS-stimulated mice, which additionally confirms their anti-inflammatory effect in mastitis. Similar results were found by Song et al. (2020a, 2020b), demonstrating that VPP and IPP reduced the protein contents of proinflammatory mediators (i.e. IL-6, IL-1 β) and chemokine MCP-1 to modulate the endothelial dysfunction caused by extracellular vesicles (EV). The anti-inflammatory function of VPP and IPP was thought to be attributed to their functional amino acid composition, such as Val and Ile. Val has been shown to exert anti-inflammatory properties via decreasing the secretion of inflammatory molecules (i.e. *IL1 β* , *IL6*, *ICAM1*, and *TNF α*) in the adipose tissues and liver (Zhou et al. 2023b). Ile has been found to exert an inhibitory effect on inflammation by modulation IL-8 generation in Caco-2 cells when induced by LPS (Garcia et al. 2024). Val and Ile released from

VPP and IPP digestion may contribute to anti-inflammatory effect (Gart et al. 2022). The inflammation in mammary gland caused by LPS also could induce neutrophil infiltration in mice (Yu et al. 2020). The decreased neutrophil infiltration of the mammary tissue in VPP and IPP group is another reason for their anti-inflammatory effects.

The β -casein is one of major components of lactogenic protein synthesized in the udder in dairy cows (Lv et al. 2020; Rehan et al. 2019). Previous studies have demonstrated that the β -casein secretion was reduced in LPS-stimulated cow mastitis (Silanikove et al. 2012). Consistent with previous studies, our findings demonstrated that LPS decreased expression of β -casein in BMECs, while VPP and IPP supplementation reversed this phenomenon. These results revealed that VPP and IPP protected the milk β -casein synthesis against the LPS-induced inflammation in mammary gland of BMECs. Moreover, the blood–milk barrier is a natural shield against external pathogens during lactation (Tsugami et al. 2017), in which key components of mammary epithelial cells are the tight junction proteins, including occludin and ZO-1 (Wellnitz et al. 2014). When stimulated by external pathogens such as LPS, the completeness of blood–milk barrier was disrupted in reaction to inflammation (Kobayashi et al. 2013). This disruption may allow more pathogens to penetrate the breast tissue from the blood to further exacerbate inflammation (Wang et al. 2017). In this study, VPP and IPP could reverse the reduced level of tight junction proteins *occludin* and *ZO1* induced by LPS, suggesting that these two peptides can maintain the integrity of blood–milk barrier and subsequently control the exacerbation of mastitis (Guo et al. 2019).

To investigate the potential molecular mechanism, RNA-seq transcriptome was employed to screen the key pathway involved in the positive effect of VPP and IPP on mammary inflammation. We found that both VPP and IPP could exert protective effects by regulating PI3K/AKT and MAPK signaling pathways in mice

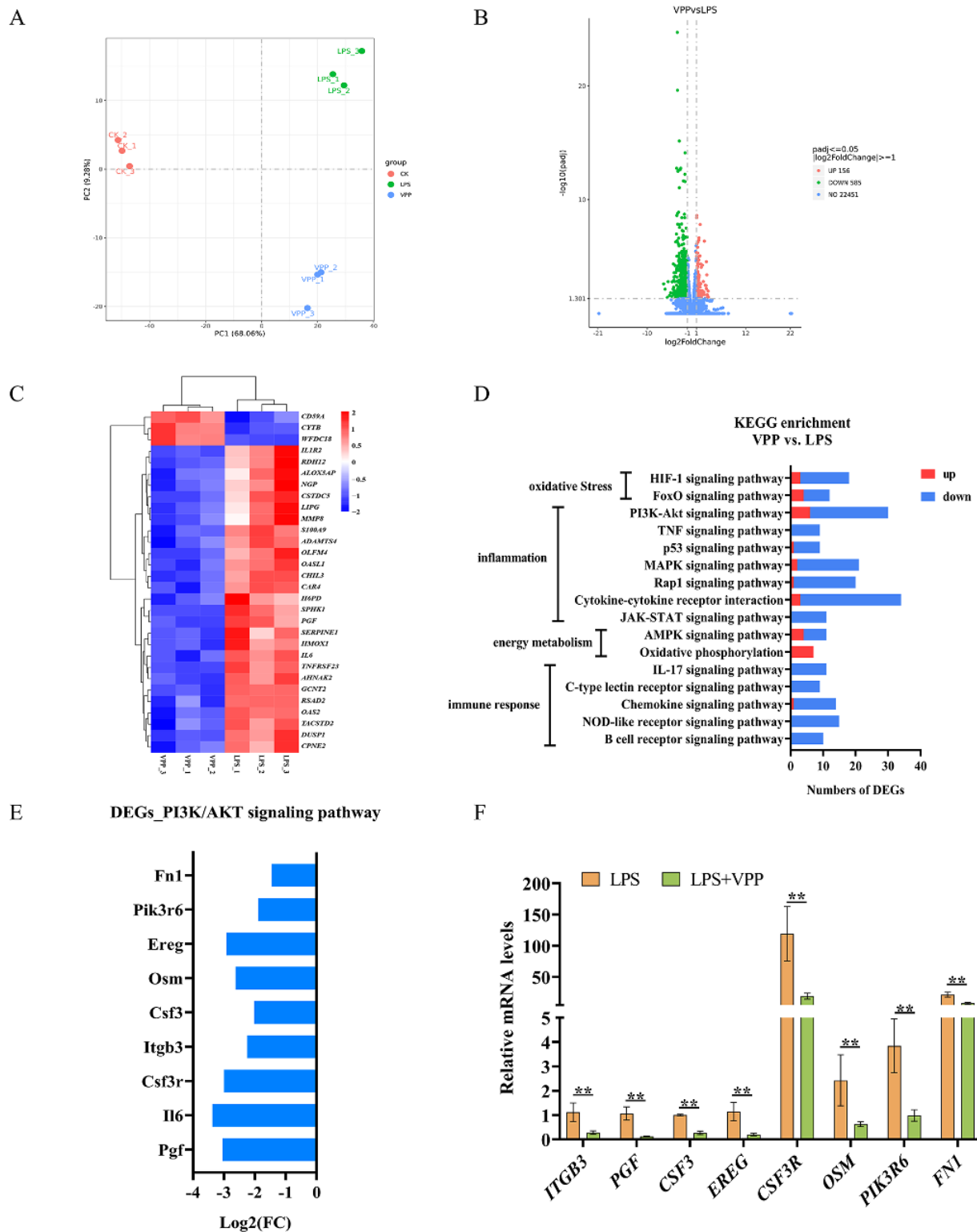


Figure 5. Transcriptome analysis of overlapping genes modified by VPP in the mammary gland of mice. (A) Principal component analysis (PCA) plot. (B) Volcano diagram. (C) Heatmap (top 30 genes with significant differences). (D) KEGG enrichment analysis. (E) DEGs enriched in PI3K/AKT signaling pathway. (F) qRT-PCR analysis. Abbreviation: CK, control.

stimulated by LPS. The pathway’s upstream target, PI3K/AKT, is essential for inflammation (Manning and Toker, 2017). Different external signals (such as TLRs, cytokines, and growth factors), activate the PI3K/AKT pathway, which subsequently specifically

causes the release of inflammatory mediators (i.e. TNF- α , IL-1 β , IL-6, etc.) and eventually enhances inflammation (Li et al. 2023, 2018). Hence, PI3K/AKT might be an important route in the development of mastitis. By stimulating the transcription

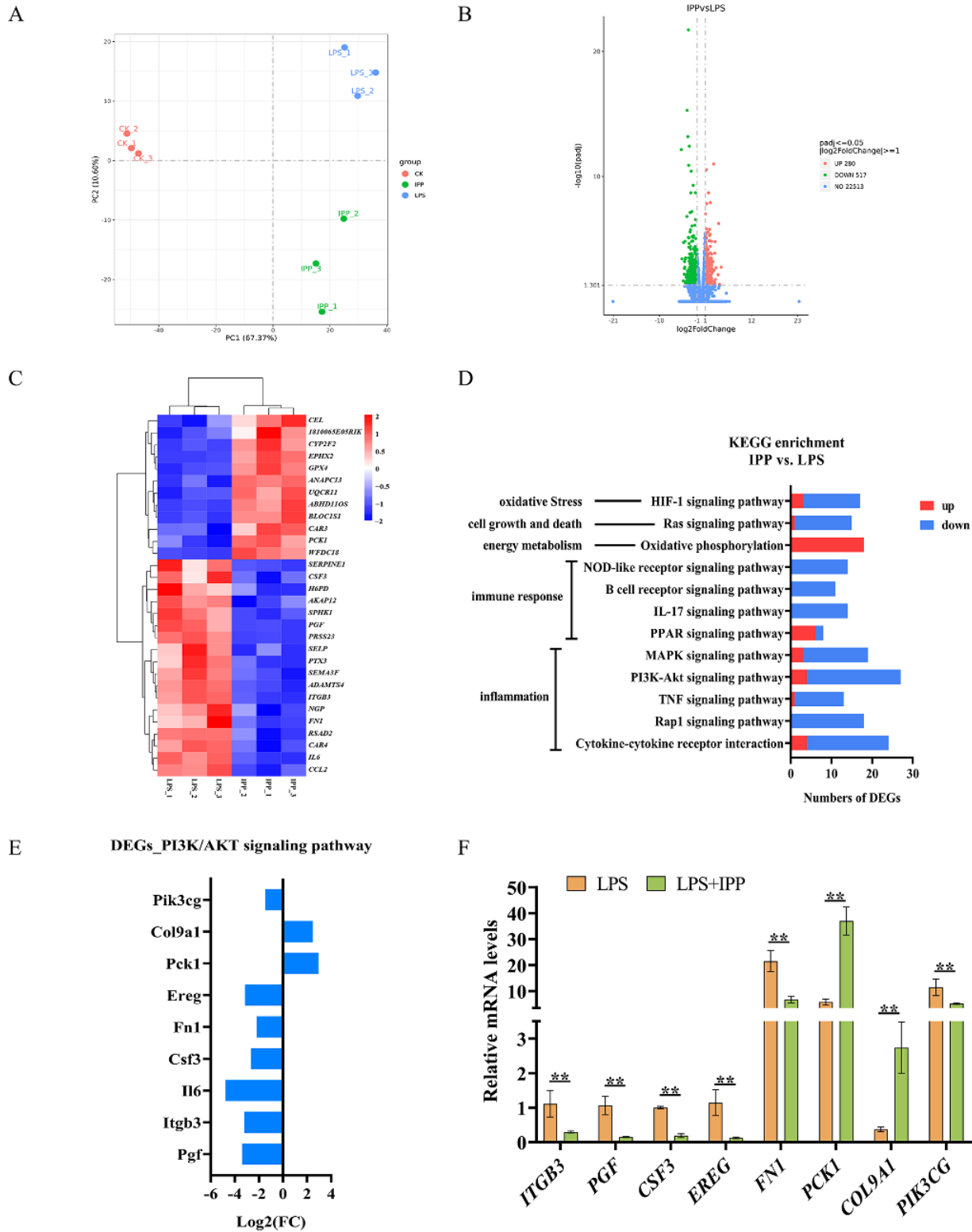


Figure 6. Transcriptome analysis of overlapping genes modified by IPP in the mammary gland of mice. (A) Principal component analysis (PCA) plot. (B) Volcano diagram. (C) Heatmap (top 30 genes with significant differences). (D) KEGG enrichment analysis. (E) DEGs enriched in PI3K/AKT signaling pathway. (F) qRT-PCR analysis. Abbreviation: CK, control.

of pro-inflammatory genes and boosting the phosphorylation of AKT, LPS stimulation can activate the PI3K/AKT signaling pathway (Chen et al. 2018). MAPK signaling pathway, one of

the principal pathways regulating inflammation, is composed of extracellular signal-regulated kinases (ERK1/2), c-JUN N-terminal kinases (JNK1/2) and p38. These components in MAPK pathway

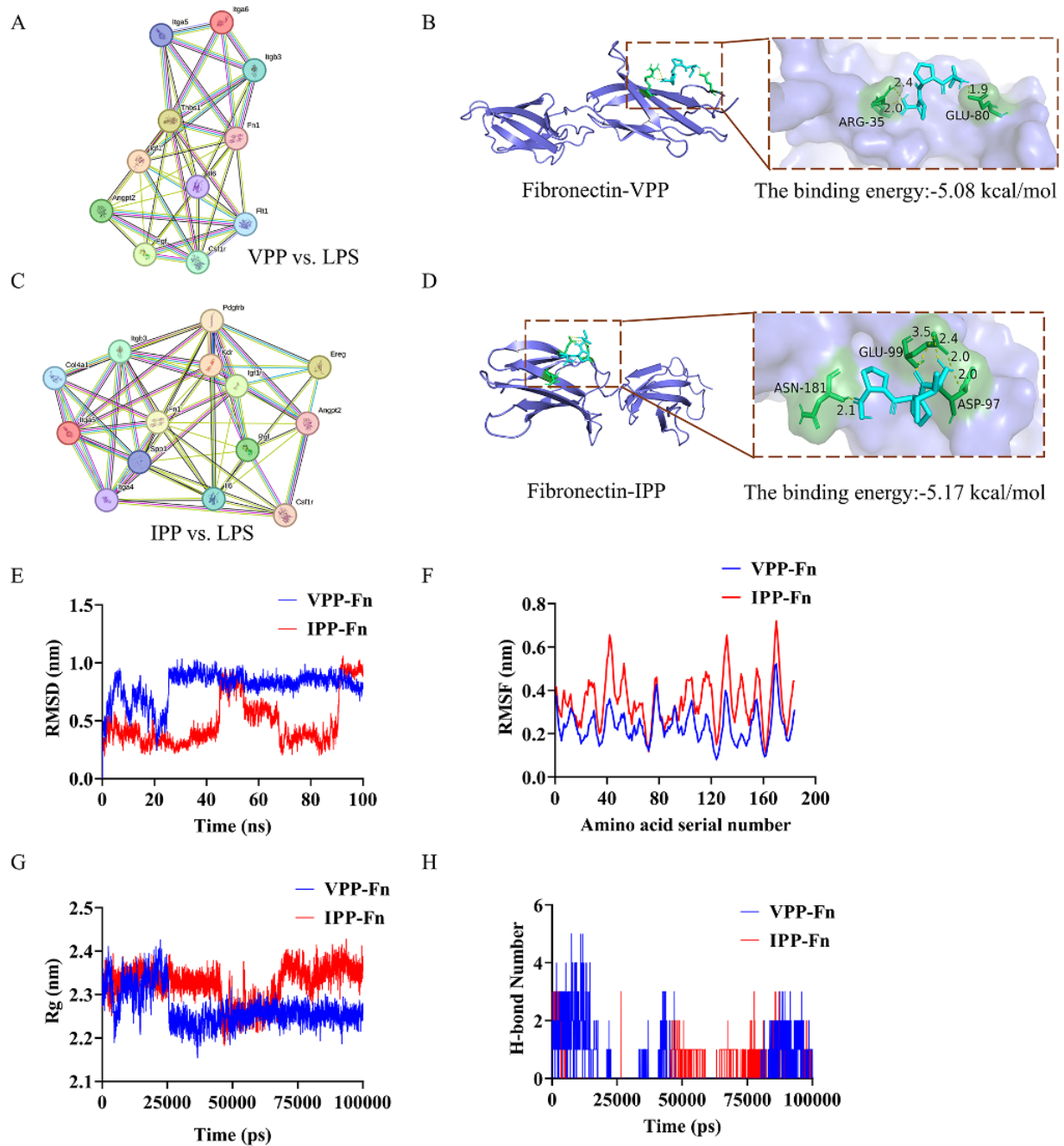


Figure 7. PPI network and molecular docking combined with molecular dynamics simulation in the VPP-fibronectin and IPP-fibronectin complexes. (A),(C) PPI network of the DEGs with a confidence score >0.7 and degree >9 in VPP and IPP compared to LPS. (B),(D) The molecular docking simulation of the binding pattern of VPP with fibronectin and IPP with fibronectin. (E) RMSD change profiles of the VPP-fibronectin and IPP-fibronectin complexes systems over time. (F) RMSF values of binding site residues in the VPP-fibronectin and IPP-fibronectin complex systems. (G) Gyration radius of the VPP-fibronectin and IPP-fibronectin complexes systems. (H) Changes in hydrogen bond number over time in the VPP-fibronectin and IPP-fibronectin complexes systems.

also can be phosphorylated by LPS stimulation and stimulate the transcription of a variety of inflammatory mediators including c-JUN, AP-1, etc (Ronkina and Gaestel, 2022). In this study, both VPP and IPP inhibited expression of key genes of PI3K-ATK and MAPK pathways, which might play a critical part in alleviating mastitis.

Fibronectin encoded by the *Fn1* gene is a part of the extracellular matrix and also is critical in signal transduction between the extracellular matrix and cell surface proteins (Liu et al. 2024).

In the current study, fibronectin is enriched in the PI3K/AKT signaling pathway which could affect proliferation of cell, inflammation, etc (Han et al. 2006). Molecular docking along with the results of molecular dynamics simulations suggested that both VPP and IPP may form stable complexes with fibronectin, providing further insight into the possible function of fibronectin in the VPP or IPP. Molecular docking showed that the binding energy of VPP-fibronectin and IPP-fibronectin were lower than -5 kcal/mol, suggesting well-being binding activity (Sohretoglu,

2018). The RMSD, RMSF, Rg, and the number of hydrogen bonds of VPP–fibronectin and IPP–fibronectin complexes were the key indicators to evaluate the stability between VPP/IPP and fibronectin (Jia et al. 2024). During simulations, RMSD can reflect the stability of peptides relevant to the protein (Sariyer et al. 2021). Global structure is more stable when the RMSD is lower. The degree of variation in the amino acid residues is shown by RMSF values (Zhou et al. 2023a). Rg may describe the density of protein structure. A lower Rg value means a more stable protein structure (Chen et al. 2020). Hydrogen bonding is an important non-covalent structural force that affects the stability of protein structures (Sohretoglu et al. 2018). Molecular docking along with the results of molecular dynamics simulations showed that VPP–fibronectin and IPP–fibronectin complexes had good binding activity. Furthermore, transcriptome results showed that VPP and IPP downregulated the expression of fibronectin which was confirmed in the qPCR results, suggesting VPP and IPP may inhibit PI3K/AKT signaling pathway through regulating fibronectin. It is reported that fibronectin activates IL-17A-mediated inflammatory pathway in EV recipient cells, promoting the secretion of proinflammatory cytokines such as IL-6 and TNF- α (Sriwastva et al. 2023). Fibronectin can stimulate the phosphorylation of AKT, the expression of which positively correlates with the activation or suppression of the PI3K/AKT pathway, which then regulates inflammation (Yang et al. 2024). In this study, fibronectin may be a potential target for VPP and IPP to reduce mammary inflammation.

Conclusion

In summary, our study suggested that milk-derived bioactive peptides VPP and IPP had a protective role against LPS-induced inflammation in BMECs and a mastitis mouse model. This anti-inflammatory activity was achieved by regulating PI3K/AKT and fibronectin may be the key target of both VPP and IPP. Furthermore, VPP and IPP also ameliorated inflammation through enhancing the blood–milk barrier in mastitis mice. These results provide innovative insights into the deeper mechanisms underlying protective effect of VPP and IPP on mastitis inflammation.

Author Contributions. Meifei Zhu and Jingyan Li contributed to the experimental design and project management; Meifei Zhu, Ruike Wei, Jingyan Li, Jiayi Bao, Lin Wei, and Xinyu Yu contributed to sample collection; Meifei Zhu and Ruike Wei analyzed data; Meifei Zhu wrote the paper; Meifei Zhu, Shanshan Li, Zheng Zhou, and Fuliang Hu revised the paper. All authors have read and approved the final manuscript.

Financial Support. This study was financially supported by National Natural Science Foundation of China (31972588), the earmarked fund for Modern Agroindustry Technology Research System from the Ministry of Agriculture of China (CARS-44), and Michigan Alliance for Animal Agriculture (AA-22-0073).

Conflicts of Interest. The authors declare no competing financial interest.

Ethical Standards. The Animal Care and Use Committee of Zhejiang Chinese Medical University (No. 86469) approved all mouse studies conducted in this work.

References

Ashraf A and Imran M (2020) Causes, types, etiological agents, prevalence, diagnosis, treatment, prevention, effects on human health and future aspects of bovine mastitis. *Animal Health Research Reviews* 21, 36–49.

- Chakrabarti S, Liao W, Davidge ST, et al. (2017) Milk-derived tripeptides IPP (Ile-Pro-Pro) and VPP (Val-Pro-Pro) differentially modulate angiotensin II effects on vascular smooth muscle cells. *Journal of Functional Foods* 30, 151–158.
- Chakrabarti S and Wu J (2015) Milk-derived tripeptides IPP (Ile-Pro-Pro) and VPP (Val-Pro-Pro) promote adipocyte differentiation and inhibit inflammation in 3T3-F442A cells. *PLoS One* 10(2), e0117492.
- Chen JG, Wu SF, Zhang QF, et al. (2020) alpha-Glucosidase inhibitory effect of anthocyanins from Cinnamomum camphora fruit: Inhibition kinetics and mechanistic insights through in vitro and in silico studies. *International Journal of Biological Macromolecules* 143, 696–703.
- Chen XX, Zheng XT, Zhang M, et al. (2018) Nuciferine alleviates LPS-induced mastitis in mice via suppressing the TLR4-NF- κ B signaling pathway. *Inflammation Research* 67(11–12), 903–911.
- Fang M, Zou T, Yang X, et al. (2021) Discovery of novel pterostilbene derivatives that might treat sepsis by attenuating oxidative stress and inflammation through modulation of MAPKs/NF-kappaB signaling pathways. *Antioxidants (Basel)* 10(9), 1333.
- Garcia BREV, Makiyama EN, Sampaio GR, et al. (2024) Effects of branched-chain amino acids on the inflammatory response induced by LPS in Caco-2 cells. *Metabolites* 14(1), 76.
- Gart E, van Duyvenvoorde W., Caspers MPM, et al. (2022) Intervention with isoleucine or valine corrects hyperinsulinemia and reduces intrahepatic diacylglycerols, liver steatosis, and inflammation in Ldlr-/-Leiden mice with manifest obesity-associated NASH. *The FASEB Journal* 36, e22435.
- Guo W, Liu B, Yin Y, et al. (2019) Licochalcone A protects the blood-milk barrier integrity and relieves the inflammatory response in LPS-induced mastitis. *Frontiers in Immunology* 10, 287.
- Han SW, Khuri FR and Roman J (2006) Fibronectin stimulates non-small cell lung carcinoma cell growth through activation of Akt/Mammalian target of Rapamycin/S6 kinase and inactivation of LKB1/AMP-activated protein kinase signal pathways. *Cancer Research* 66(1), 315–323.
- Huang FQ, Teng KL, Liu YY, et al. (2022) Nisin Z attenuates lipopolysaccharide-induced mastitis by inhibiting the ERK1/2 and p38 mitogen-activated protein kinase signaling pathways. *Journal of Dairy Science* 105, 3530–3543.
- Jia R, Yang Y, Liao GZ, et al. (2024) Flavor characteristics of umami peptides from wuding chicken revealed by molecular dynamics simulation. *Journal of Agricultural and Food Chemistry* 72(7), 3673–3682.
- Jiang MC, Lv ZY, Huang YH, et al. (2022) Quercetin alleviates lipopolysaccharide-induced inflammatory response in bovine mammary epithelial cells by suppressing TLR4/NF- κ B Signaling Pathway. *Frontiers in Veterinary Science* 9, 915726.
- Kobayashi K, Oyama S, Numata A, et al. (2013) Lipopolysaccharide disrupts the milk-blood barrier by modulating claudins in mammary alveolar tight junctions. *Plos One* 8, e62187.
- Li B, Xi PP, Wang ZL, et al. (2018) PI3K/Akt/mTOR signaling pathway participates in *Streptococcus uberis*-induced inflammation in mammary epithelial cells in concert with the classical TLRs/NF- κ B pathway. *Veterinary Microbiology* 227, 103–111.
- Li KF, Ran X, Zeng YR, et al. (2023) Maslinic acid alleviates LPS-induced mice mastitis by inhibiting inflammatory response, maintaining the integrity of the blood-milk barrier and regulating intestinal flora maslinic acid. *International Immunopharmacology* 122, 110551.
- Li SS, Bu TT, Zheng JX, et al. (2019) Preparation, bioavailability, and mechanism of emerging activities of Ile-Pro-Pro and Val-Pro-Pro. *Comprehensive Reviews in Food Science and Food Safety* 18(4), 1097–1110.
- Li Y, Shao J, Hou P et al. (2021) Nrf2-ARE signaling partially attenuates lipopolysaccharide-induced mammary lesions via regulation of oxidative and organelle stresses but not inflammatory response in mice. *Oxidative Medicine and Cellular Longevity*, 8821833.
- Liu XJ, Li SS, Zou YX, et al. (2018) Lysine stimulates protein synthesis by promoting the expression of ATB0,+ and activating the mTOR pathway in bovine mammary epithelial cells. *The Journal of Nutrition* 148(9), 1426–1433.
- Liu L, Hong YT, Ma C et al. (2024) Circular RNA Gtdc1 protects against offspring osteoarthritis induced by prenatal prednisone exposure by regulating SRSF1-Fn1 signaling. *Advanced Science* 202307422.

- Liu L, Yu SF, BU TT, *et al.* (2023) Casein hydrolysate alleviates adipose chronic inflammation in high fat-diet induced obese C57BL/6J mice through MAPK pathway. *Nutrients* **15**(8), 1813.
- Lv Z, Liu H, Yang Y, *et al.* (2020) Changes in metabolites from bovine milk with β -casein variants revealed by metabolomics. *Animals* **10**, 954.
- Manning BD and Toker A (2017) AKT/PKB signaling: navigating the network. *Cell* **169**(3), 381–405.
- Nakamura Y, Yamamoto N, Sakai K, *et al.* (1995) Antihypertensive effect of sour milk and peptides isolated from it that are inhibitors to angiotensin I-converting enzyme. *Journal of Dairy Science* **78**(6), 1253–1257.
- Ran X, Liu JX, Fu SP, *et al.* (2022) Phytic acid maintains the integrity of the blood–milk barrier by regulating inflammatory response and intestinal flora structure. *Journal of Agriculture and Food Chemistry* **70**(1), 381–391.
- Ran X, Yan Z, Yang Y, *et al.* (2020) Dioscin improves pyroptosis in LPS-induced mice mastitis by activating AMPK/Nrf2 and inhibiting the NF-kappaB signaling pathway. *Oxidative Medicine and Cellular Longevity* **8845521**.
- Rehan F, Ahemad N, Gupta M, *et al.* (2019) Casein nanomicelle as an emerging biomaterial—A comprehensive review. *Colloids and Surfaces B: Biointerfaces* **179**, 280–292.
- Ronkina N and Gaestel M (2022) MAPK-activated protein kinases: Servant or partner? *Annual Review of Biochemistry* **91**, 505–540.
- Sariyer E, Kocer S, Danis O, *et al.* (2021) In vitro inhibition studies of coumarin derivatives on *Bos Taurus* enolase and elucidating their interaction by molecular docking, molecular dynamics simulations and MMGB(PB)SA binding energy calculation. *Bioorganic Chemistry* **110**, 104796.
- Sawada Y, Sakamoto Y, Toh M, *et al.* (2015) Milk-derived peptide Val-Pro-Pro (VPP) inhibits obesity-induced adipose inflammation via an angiotensin-converting enzyme (ACE) dependent cascade. *Molecular Nutrition and Food Research* **59**(12), 2502–2510.
- Sharun K, Dhama K, Tiwari R, *et al.* (2021) Advances in therapeutic and management approaches of bovine mastitis: A comprehensive review. *Veterinary Quarterly* **41**(1), 107–136.
- Silanikove N, Rauch-Cohen A, Shapiro F, *et al.* (2012) Lipopolysaccharide challenge of the mammary gland in cows induces nitrosative stress that impairs milk oxidative stability. *Animal* **6**(9), 1451–1459.
- Sohretoglu D, Sari S, Soral M, *et al.* (2018) Potential of *Potentilla inclinata* and its polyphenolic compounds in α -glucosidase inhibition: Kinetics and interaction mechanism merged with docking simulations. *International Journal of Biological Macromolecules* **108**, 81–87.
- Song TY, Lv M, Zhang L, *et al.* (2020a) The protective effects of tripeptides VPP and IPP against small extracellular vesicles from angiotensin II-induced vascular smooth muscle cells mediating endothelial dysfunction in human umbilical vein endothelial cells. *Journal of Agricultural and Food Chemistry* **68**(47), 13730–13741.
- Song TY, M. L, Sun BG, *et al.* (2020b) Tripeptides Val-Pro-Pro (VPP) and Ile-Pro-Pro (IPP) regulate the proliferation and migration of vascular smooth muscle cells by interfering ang ii-induced human umbilical vein endothelial cells derived evs delivering RNAs to VSMCs in the co-culture model. *Journal of Agricultural and Food Chemistry* **68**(24), 6628–6637.
- Sriwastva MK, Teng Y, Mu JY, *et al.* (2023) An extracellular vesicular mutant KRAS-associated protein complex promotes lung inflammation and tumor growth. *Journal of Extracellular Vesicles* **12**(2), 12307.
- Tsugami Y, Matsunaga K, Suzuki T, *et al.* (2017) Phytoestrogens weaken the blood-milk barrier in lactating mammary epithelial cells by affecting tight junctions and cell viability. *Journal of Agricultural and Food Chemistry* **65**, 11118–11124.
- Wan J, Zhang YY, Yang DQ, *et al.* (2021) Gastrodin improves nonalcoholic fatty liver disease through activation of the adenosine monophosphate-activated protein kinase signaling pathway. *Hepatology* **74**(6), 3074–3089.
- Wang JJ, Wei ZK, Zhang X, *et al.* (2017) Butyrate protects against disruption of the blood-milk barrier and moderates inflammatory responses in a model of mastitis induced by lipopolysaccharide. *British Journal of Pharmacology* **174**, 3811–3822.
- Wellnitz O, Wall SK, Saudenova M, *et al.* (2014) Effect of intramammary administration of prednisolone on the blood-milk barrier during the immune response of the mammary gland to lipopolysaccharide. *Am J Vet Res* **75**, 595.
- Yang B, Shen FX, Zhu Y, *et al.* (2024) Downregulating ANGPTL3 by miR-144-3p promoted TGF- β 1-induced renal interstitial fibrosis via activating PI3K/AKT signaling pathway. *Heliyon* **10**(3), e24204.
- Yang G, Yue Y, Li D, *et al.* (2020) Antibacterial and immunomodulatory effects of pheromonicin-NM on *Escherichia coli*-challenged bovine mammary epithelial cells. *International Immunopharmacology* **84**, 106569.
- Yin H, Xue G, Dai A *et al.* (2021) Protective effects of lentinan against lipopolysaccharide-induced mastitis in mice. *Frontiers in Pharmacology* **12**, 755768. 10.3389/fphar.2021.755768
- Yu S, Liu X, Yu D, *et al.* (2020) Piperine protects LPS-induced mastitis by inhibiting inflammatory response. *International Immunopharmacology* **87**, 106804.
- Zhou H, Bie S, Li J, *et al.* (2023a) Comparison on inhibitory effect and mechanism of inhibitors on sPPO and mPPO purified from ‘Lijiang snow’ peach by combining multispectroscopic analysis, molecular docking and molecular dynamics simulation. *Food Chemistry* **400**, 134048.
- Zhou XB, Zhang JJ, Shen J, *et al.* (2023b) Branched-chain amino acid modulation of lipid metabolism, gluconeogenesis, and inflammation in a finishing pig model: Targeting leucine and valine. *Food & Function* **14**, 10119–10134.